CS — Copy given this to me @ POAC '85 Narssarssuaq Greenland

J.B. Johnson
G.F.N. Cox
W.B. Tucker

U.S. Army Cold Regions Research and Engineering Laboratory
Hanover, New Hampshire, USA

KADLUK ICE STRESS MEASURMENT PROGRAM

Abstract

Cylindrical biaxial stress sensors were used to measure ice stress variations as a function of depth across an ice peninsula on the shoreward side (south) of Kadluk Island. The stresses varied in a complex manner both laterally and with depth in the ice sheet. Average stresses were calculated and summed across the ice peninsula to determine the ice load acting on the structure. The maximum measured average stress and corresponding calculated structural load during the experiment were about 300 kPa and 150 MN respectively. All significant measured stresses were caused by thermal expansion of the ice sheet.

1 INTRODUCTION

Estimates of the magnitude of ice forces on offshore arctic structures can be obtained from analytical models, scale model tests, and field measurements. Unfortunately, analytical models and model tests usually only provide upper bound ice load estimates. In such models conservative assumptions are made to compensate for a lack of understanding of the ice failure mode and the large-scale mechanical properties of the ice cover. Field measurements of ice stress are needed to obtain actual ice loads on structures and for model tuning and verification. While the measurement of extreme ice stress events is not usually possible, data at lower stresses are very useful for understanding the vertical and lateral stress distribution in the ice sheet, non-simultaneous failure across the full width of the

structure, and the relationship between the local stress and far-field geophysical stress.

During the spring of 1984, eighteen biaxial ice stress sensors were deployed at six sites near Esso's caisson retained island in Mackenzie Bay, Canada. In addition to measuring ice stress and ice temperature, ice movement and wind speed and direction were also monitored by Esso. This paper summarizes our findings on the variation of ice stress in the ice sheet and examines the environmental driving forces during the program. Results from several biaxial ice stress sensors are also compared to stress measurements obtained from an Exxon Production Research (EPR) stress panel. A more detailed discussion of the sensor, field program, and results can be found in Cox et al. /4/.

2 FIELD PROGRAM

2.1 Site Description

The caisson retained island (CRI) was located on a man-made berm in 14.5 m of water at Esso's Kadluk location in Mackenzie Bay (Fig. 1). The CRI consisted of eight caissons connected

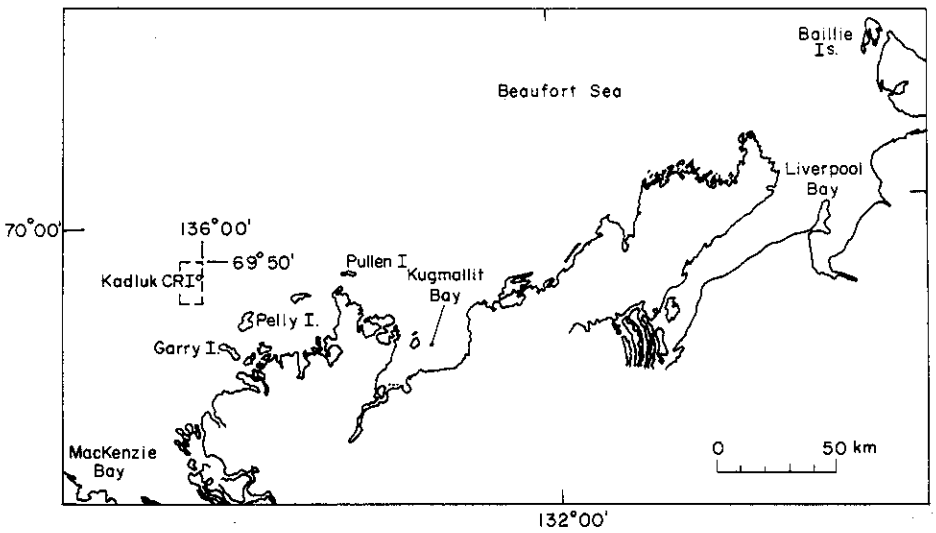

Fig. 1. Kadluk ice stress measurement program location.

Fig. 2. Caisson retained island, ice island, and surrounding ice conditions before March 12.

together by steel cables to form an octagonal ring 12.2 m high and 117 m in diameter (Fig. 2) /7/. Esso also constructed a man-made ice island on the north side of the CRI to serve as an emergency relief well drill site.

At the time of our deployment during the first week of March, there was an extensive grounded rubble field on the southwest side of the CRI and ice island (Fig. 4). The surrounding first-year sea ice was about 1.7 m thick. A few small grounded multi-year floes were also observed on the east side of the caisson and between the caisson and ice island.

2.2 Sensor Placement

It was originally planned to deploy the sensors at eight sites around the CRI-ice island-rubble complex. With this deployment scheme it would be possible to determine the total ice load on the complex regardless of the direction of ice movement. However, on March 11, just as we were completing our installation, strong southerly winds caused the ice on the north side of

Fig. 3. Ice conditions around CRI after March 12.

the complex to break away and move out to sea. The CRI-ice island-rubble area was left as a peninsula on the edge of the inshore fast ice (Fig. 3). Even though we lost most of our cable we were able to recover all of our sensors for a second deployment.

The second deployment was on the south side of the CRI and rubble and took place in the two stages. During the first stage on March 12, stress sensors were installed at Sites 1 and 3 (Fig. 4). At Site 1 sensors were placed at depths of 10, 42, and 109 cm in the ice, while at Site 3 only one sensor was installed at 10 cm. A thermistor string was also placed in the ice sheet to provide continuous temperature data.

The remaining ice stress sensors were installed during the first week of April after we had obtained additional cable and had an opportunity to evaluate the ice conditions on the north side of the complex. As the ice on the north side remained thin and continued to move offshore, it was decided to deploy all of the sensors on the south side. The sensors at Sites 1 and 3 were

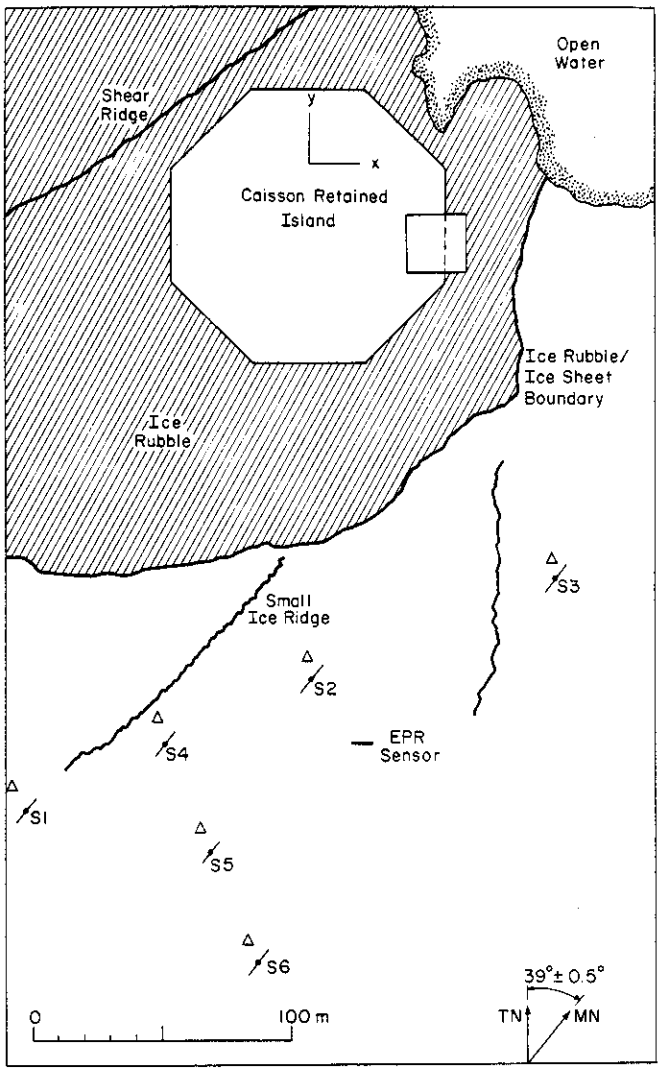

Fig. 4. Stress measurement site locations. The slashed dots show the positions of the sensors on April 12 and the triangles show the positions of the sensors on May 4.

reinstalled and four more sites were added to the array (Fig. 4). At each of the six sites stress sensors were installed at depths of 30, 80, and 130 cm. The sensors were positioned to allow us to calculate the ice load on the CRI and rubble (Sites 1, 2, 3, and 4), to detect bending in the ice sheet (Sites 4, 5, and 6), and to evaluate the vertical and lateral variations in ice stress magnitude and direction. The second deployment was completed and became operational on April 9.

2.3 Ice Stress Sensors

The biaxial ice stress sensor consists of a stiff cylinder made of steel. Principal ice stresses normal to the axis of the gauge are determined by measuring the radial deformation of the cylinder in three directions using vibrating-wire technology. A detailed discussion of the sensor design and performance can be found in Cox and Johnson /1,3/. The sensor has successfully been used to measure thermal ice pressures in New Hampshire lakes /2/ and ice forces on Adams Island in the Canadian Arctic /5/.

3 FIELD PROGRAM RESULTS

Page limitations prevent us from presenting the output from all the stress sensors. However, most of our findings can be illustrated in a few figures. Figures 5 and 6 show how the magnitude and direction of ice stress vary with depth. The results shown in Figure 5 are from Site 1 and were obtained during the latter part of March. The results shown in Figure 6 are from Site 3

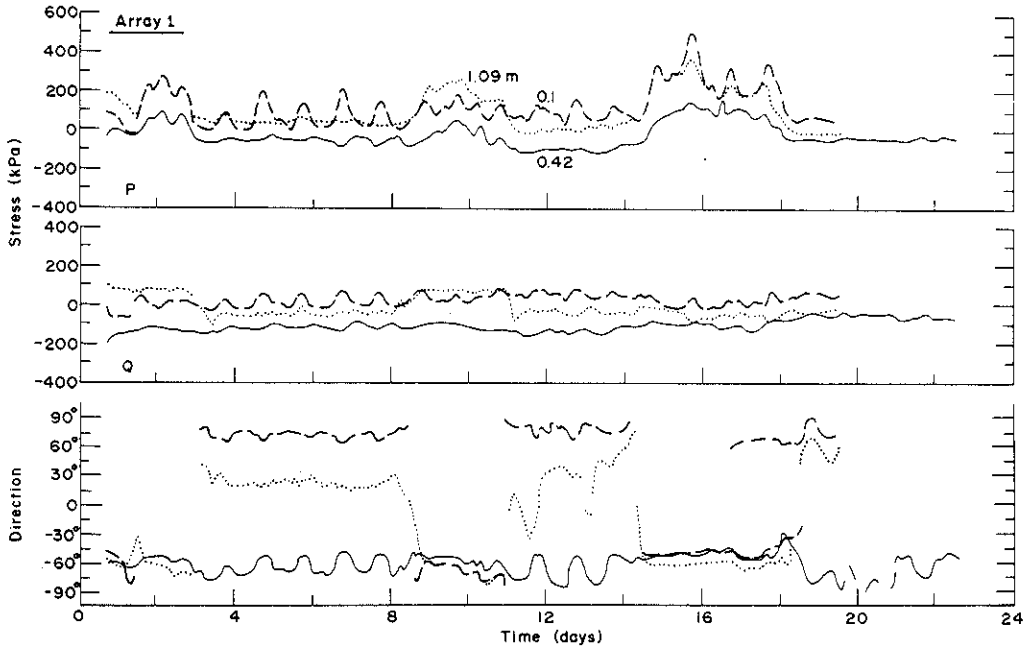

Fig. 5. Vertical variation of ice stress at Site 1 during the latter part of March. Day 0 corresponds to March 12.

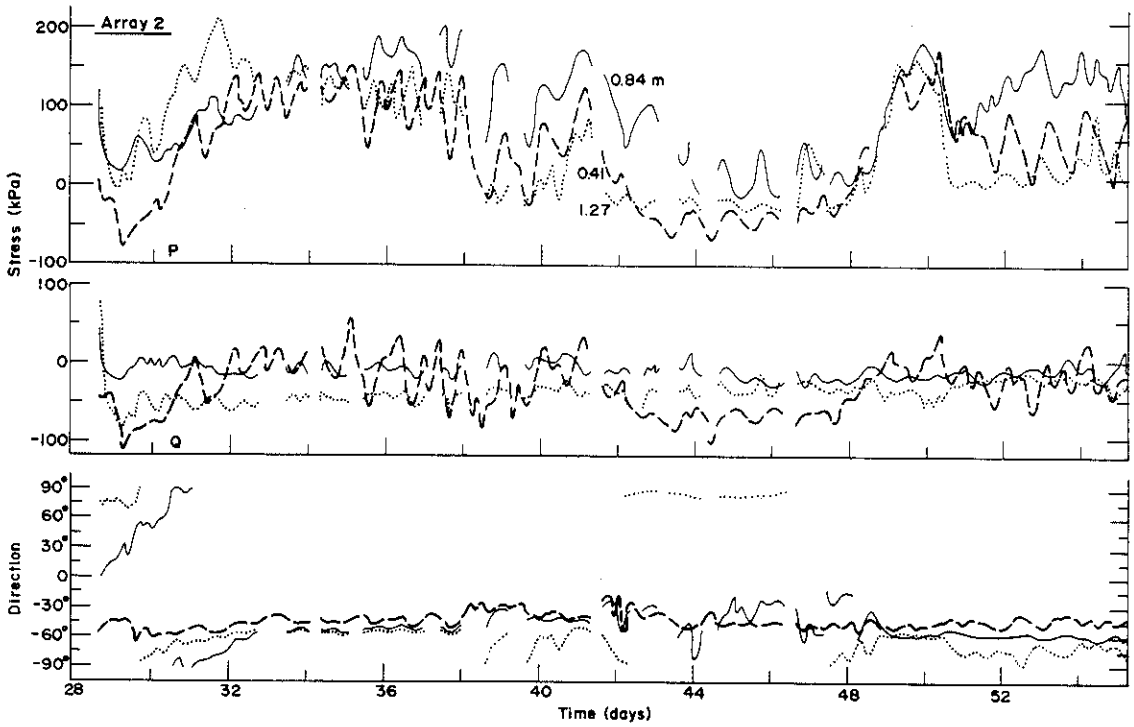

Fig. 6. Vertical variation of ice stress at Site 3 during April and early May.

and were obtained in April and early May. In these two figures, P and Q are the principal stresses where a positive stress value indicates compression. θ is the angle measured counterclockwise from the principal stress direction P to magnetic north. Figure 7 shows the lateral variation in the average normal and shear stresses at different times in front of the CRI and rubble. Here, σ_y is the true north component of the average stress in the top, middle and bottom of the ice sheet; σ_x is the true east component; and τ_{xy} is the corresponding average shear stress. The average stresses were determined by first calculating the normal and shear stresses at each depth from P, Q, and θ using Mohr circle theory. These values were then weighted according to the sensor position in the ice sheet and summed to obtain the average full thickness ice stress values.

The positions of the ice stress sensor sites were surveyed on April 12 and May 4. During this period the ice moved about 10 m towards the CRI and rubble (Fig. 4). Detailed ice movement measurements from February 22 to May 23, obtained for Esso by

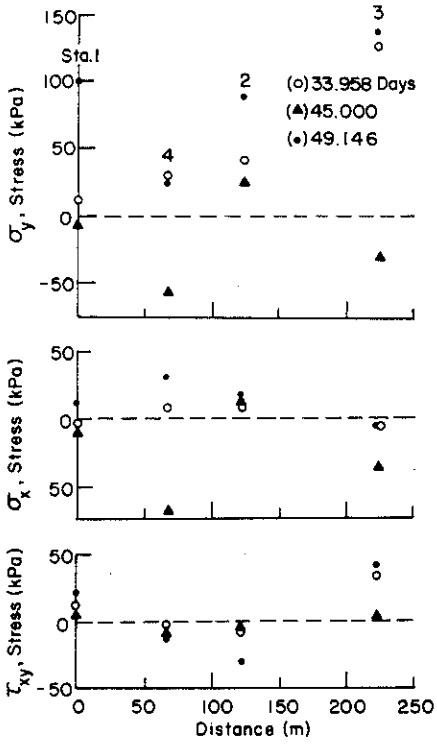

Fig. 7. Lateral variation of average normal and shear stresses at selected times.

Oceanographic Services, Inc. /8/, are not presented here because of space limitations, but are summarized in Cox et al. /4/. Wind and ice temperature data are plotted in Figure 9.

4 DISCUSSION

It is evident from Figures 5 and 6 that the vertical stress distribution in an ice sheet can be complex. Contrary to our expectations /5/, maximum stresses were not only observed in the top part of the ice sheet, but also in the middle and bottom of the ice sheet at different times. Secondary principal stresses were usually much smaller. During significant stress events (> 100 kPa), the principal stress directions tended to be aligned in the top, middle, and bottom of the ice sheet, whereas during relatively quiet periods (< 100 kPa), the stress directions varied considerably with depth. Stresses at all depths also varied in a cyclic manner, in response to diurnal fluctuations in the air and ice temperatures.

The maximum measured compressive stress was about 500 kPa. This stress was measured in the top portion of the ice sheet at Site 1 on 27 March. The corresponding average full thickness ice stress at this site was about 300 kPa. Tensile stresses were always lower than 140 kPa, and may be a measure of the large-scale tensile strength of the ice cover.

The complexity of the vertical stress distribution suggests that the ice sheet was in a state of bending and superimposed on the bending stresses, we also had local thermal stresses. This is probabably reasonable, in that upward and downward bending of the ice sheet was observed along rubble pile in front of the structure. Flexure failure of the ice sheet at the rubble pile would also explain the relatively low measured ice stress values.

Lateral variations in stress at any given level were equally complex and may also be a reflextion of upward and downward bending of the ice sheet along the length of the rubble pile. However, during significant stress events, the average full thickness ice stress did show a strong tendency to increase, from west to east, along our measurement line (Fig. 7). This may have been due to the presence of grounded multi-year ice features at the east end of our line of sensors. During quiet periods, there were no consistent lateral variations in the average stress.

An EPR ice pressure panel was installed by Esso on the south side of the structure, about 20 m from Site 2. The panel face was oriented about 6° east of true north. Figure 8 shows how our average full thickness stress measurements compare to that obtained by the EPR panel. The agreement between the two types of sensors is quite good, particularly between the EPR panel and our sensors at Site 2, only 20 m away. During the first part of the program we only had an array of sensors at Site 1 and our measurements are somewhat lower than those obtained by the panel. This is not surprising, in that Site 1 was located 150 m

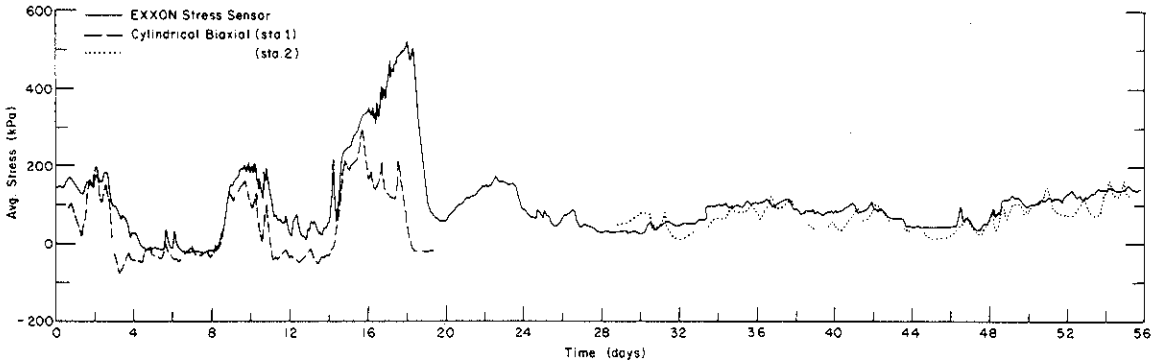

Fig. 8. Comparison between data obtained from several biaxial ice stress sensors and the EPR ice pressure panel.

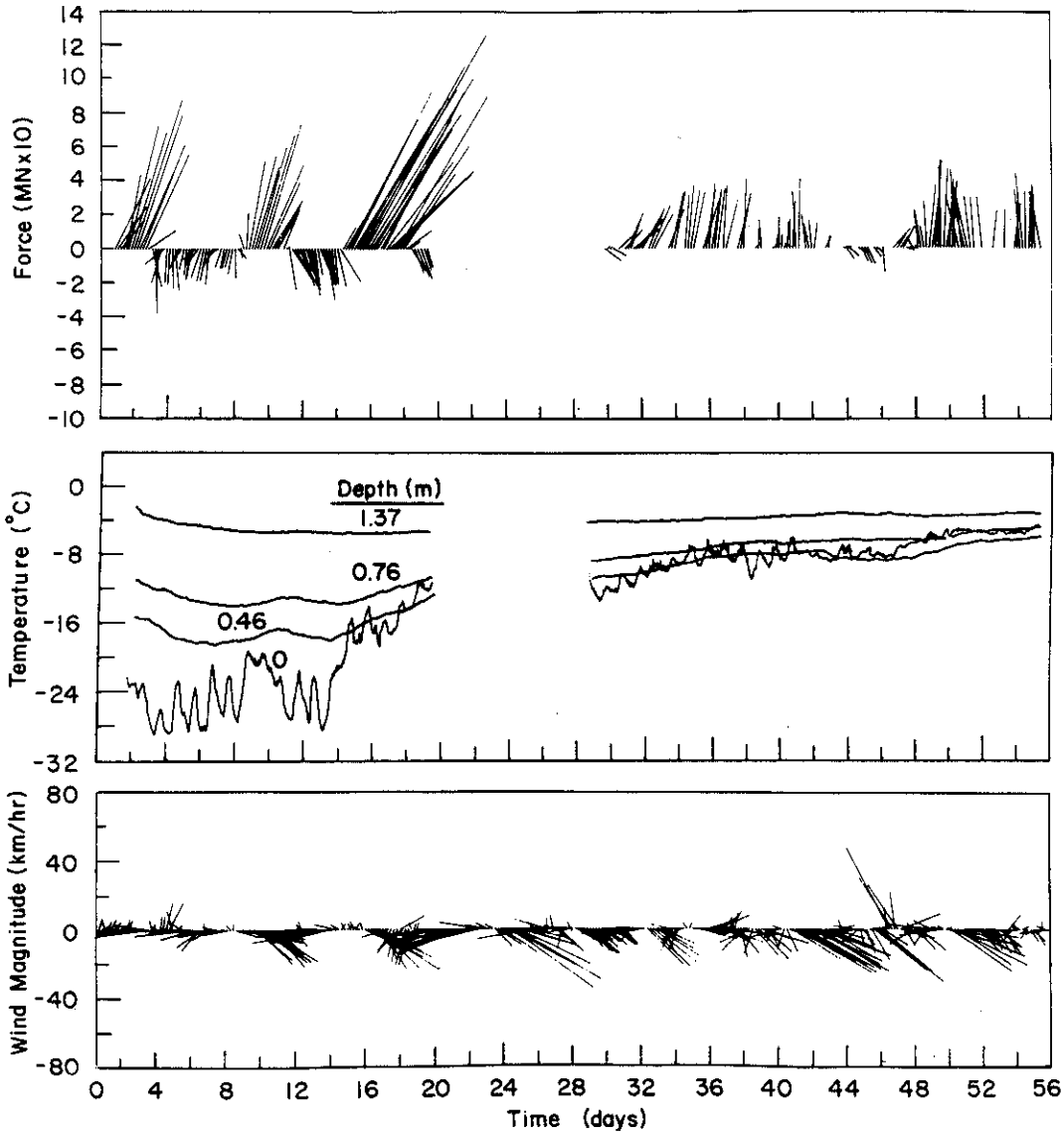

Fig. 9. Ice forces acting on CRI-ice island-rubble complex, ice temperature, and wind data for measurement program.

to the west of the panel, and our later measurements show an increase in ice stress from west to east.

The average normal and shear stress measurements at Sites 1, 2, 3, and 4 were used to calculate the total ice load on the CRI and rubble /4,6/. The results are presented in Figure 9 along with the ice temperature and wind data acquired during the study. The force acting across the peninsula on the south side of the island and wind speed and direction are given in the form of vector stick plots. The force vectors point in the direction of the applied load and the wind vectors point in the direction the wind was blowing to. The maximum calculated load was 150 MN.

The ice load, ice temperature, and wind data indicate that all significant ice stress events were of thermal origin. During periods of high stress, winds were predominantly blowing to the south, while the forces were toward the north. The high stress periods actually correspond very well to periods of ice sheet warming. The stresses are produced by the seaward motion of the ice as a result of the expansion of the ice sheet between the structure and the coastline /9/.

5 CONCLUSIONS

Cylindrical biaxial ice stress sensors were used to measure the ice stress variations as a function of depth across an ice peninsula on the shoreward (south) side of Esso's Kadluk caisson retained island. The stresses varied in a complex manner both laterally and with depth in the ice sheet. The stress data and field observations suggest that the ice sheet was in a state of bending and superimposed on the bending stresses we also had local thermal stresses. During significant stress events (> 100 kPa) the principal stress directions in the top, middle, and bottom of the ice sheet were aligned and average normal stresses in the ice increased from west to east along our line of sens-

ors. During relatively quiet periods, no systematic variations in either the vertical or lateral stresses were noted. The maximum measured compressive stress between mid-March and early May was about 500 kPa. This stress was measured in the top portion of the ice sheet during a period of ice sheet warming. The corresponding average full thickness ice stress at this site was 300 kPa. The data from the biaxial ice stress sensors agreed reasonably well with average stress data obtained from an EPR ice pressure panel.

6 ACKNOWLEDGEMENTS

This work was sponsored by the Minerals Management Service (MMS) of the U.S. Department of the Interior with logistic and technical support from Esso Resources Canada (ERC). The authors are particularly grateful to Bill Bosworth of CRREL, Charlie Smith of MMS, and Rick Wards of ERC for their assistance in the field program planning and execution. We also thank Gary Decoff and Dianne Ronan of CRREL for managing our extensive data base during our analyses.

7 REFERENCES

1. COX, G.F.N., Evaluation of a biaxial ice stress sensor. IAHR Ice Sympsoium, Hamburg, 1984. Vol. 2, pp. 340-361.

2. COX, G.F.N., A preliminary investigation of thermal ice pressures. Cold Regions Science and Technology, Vol. 9, 1984, pp. 221-229.

3. COX, C.F.N. and JOHNSON, J.B., Stress measurements in ice. U.S. Army Cold Regions Research and Engineering Laboratory, Research Report 83-23, 31 p.

4. COX, G.F.N.; JOHNSON, J.B.; TUCKER, W.B. and BOSWORTH, H.W., Kadluk ice stress measurement program. U.S. Army Cold Regions Research and Engineering Laboratory, Research Report, in preparation.

5. FREDERKING, R.M.W.; SAYED, M.; WESSELS, E.; CHILD, A.J.; and BRADFORD, D., Ice interaction with Adams Island, winter 1982-83. IAHR Ice Symposium, Hamburg 1984, in press.

6. JOHNSON, J.B., A surface integral method for determining ice loads on offshore structures from in situ measurements. Annals of Glaciology, Vol. 4, 1983, pp. 124-128.

7. MANCINI, C.V.; DOWSE, B.E.W. and CHEVALLIER, J-M, Caisson retained island for Canadian Beaufort Sea - Geotechnical design and construction considerations. Offshore Technology Conference Paper 4581, Houston 1983. Vol. 4, pp. 17-22.

8. OCEANOGRAPHIC SERVICES, INC., Kadluk Island ice movement 1984. OSI#5586, Santa Barbara, CA, June 1984, 62 p.

9. SANDERSON, T.J.O., Thermal ice forces against isolated structures. IAHR Ice Symposium, Hamburg 1984, in press.